






## Strengthening the Link Between Fullerenes and a Subset of Diffuse Interstellar Bands

DANIEL MAJAESS <sup>1</sup>, TINA A. HARRIOTT <sup>2,1</sup>, HALIS SEURET<sup>3,1</sup>, CERCIS MORERA-BOADO <sup>4</sup>,  
LOU MASSA <sup>5</sup>, AND CHÉRIF F. MATTA <sup>1,6,7,8</sup>

<sup>1</sup>Department of Chemistry and Physics, Mount Saint Vincent University, Halifax, Nova Scotia, B3M2J6 Canada.

<sup>2</sup>Department of Mathematics and Statistics, Mount Saint Vincent University, Halifax, Nova Scotia, B3M2J6 Canada.

<sup>3</sup>Centro de Investigaciones Químicas, IICBA, Universidad Autónoma del Estado de Morelos, Cuernavaca, 62209, Morelos, Mexico.

<sup>4</sup>IXM-Cátedra Conahcyt-Centro de Investigaciones Químicas, IICBA, Universidad Autónoma del Estado de Morelos, Cuernavaca, 62209, Morelos, Mexico.

<sup>5</sup>Hunter College & the PhD Program of the Graduate Center, City University of New York, New York, USA.

<sup>6</sup>Department of Chemistry, Saint Mary's University, Halifax, Nova Scotia, B3H3C3 Canada.

<sup>7</sup>Département de Chimie, Université Laval, Québec, G1V0A6 Canada.

<sup>8</sup>Department of Chemistry, Dalhousie University, Halifax, Nova Scotia, B3H4J3 Canada.

### ABSTRACT

A debate persists regarding the correlation between the DIBs 9577 and 9632 Å, and whether they share a common molecular carrier (i.e., C<sub>60</sub><sup>+</sup>). A robust high correlation determination emerges after bridging the baseline across an order of magnitude ( $\simeq 50 - 700$  mÅ,  $r = 0.93 \pm 0.02$ ), and nearly doubling the important higher equivalent width domain by adding new Mg II-corrected sightlines. Moreover, additional evidence is presented of possible DIB linkages to fullerenes, whereby attention is drawn to DIBs at 7470.38, 7558.44, and 7581.47 Å, which match the Campbell experimental results for C<sub>70</sub><sup>+</sup> within 1 Å, and the same is true of 6926.48 and 7030.26 Å for C<sub>70</sub><sup>2+</sup>. Yet their current correlation uncertainties are unsatisfactory and exacerbated by expectedly low EWs (e.g.,  $\overline{EW} = 4$  mÅ for 6926.48 Å), and thus further observations are required to assess whether they represent a *bona fide* connection or numerical coincidence.

*Keywords:* Astrochemistry (75)

### 1. INTRODUCTION

Galazutdinov et al. (2017, 2021), Schlarmann et al. (2021), and Nie et al. (2022) debated the correlation between the 9577 and 9632 Å DIBs, which experiments highlight as prominent absorption features associated with C<sub>60</sub><sup>+</sup> (e.g., Fullara et al. 1993; Campbell et al. 2015). Galazut-

dinov et al. (2021) argued those DIBs exhibit too low a correlation to be associated, or an unknown causes the correlation to vary (e.g., blended lines). Conversely, Schlarmann et al. (2021) and Nie et al. (2022) favored a high correlation and unambiguous link to C<sub>60</sub><sup>+</sup>. DIBs tied to 9365.2 and 9427.8 Å may also be associated with C<sub>60</sub><sup>+</sup> (Campbell et al. 2016a; Walker et al. 2016; Lallement et al. 2018; Cordiner et al.

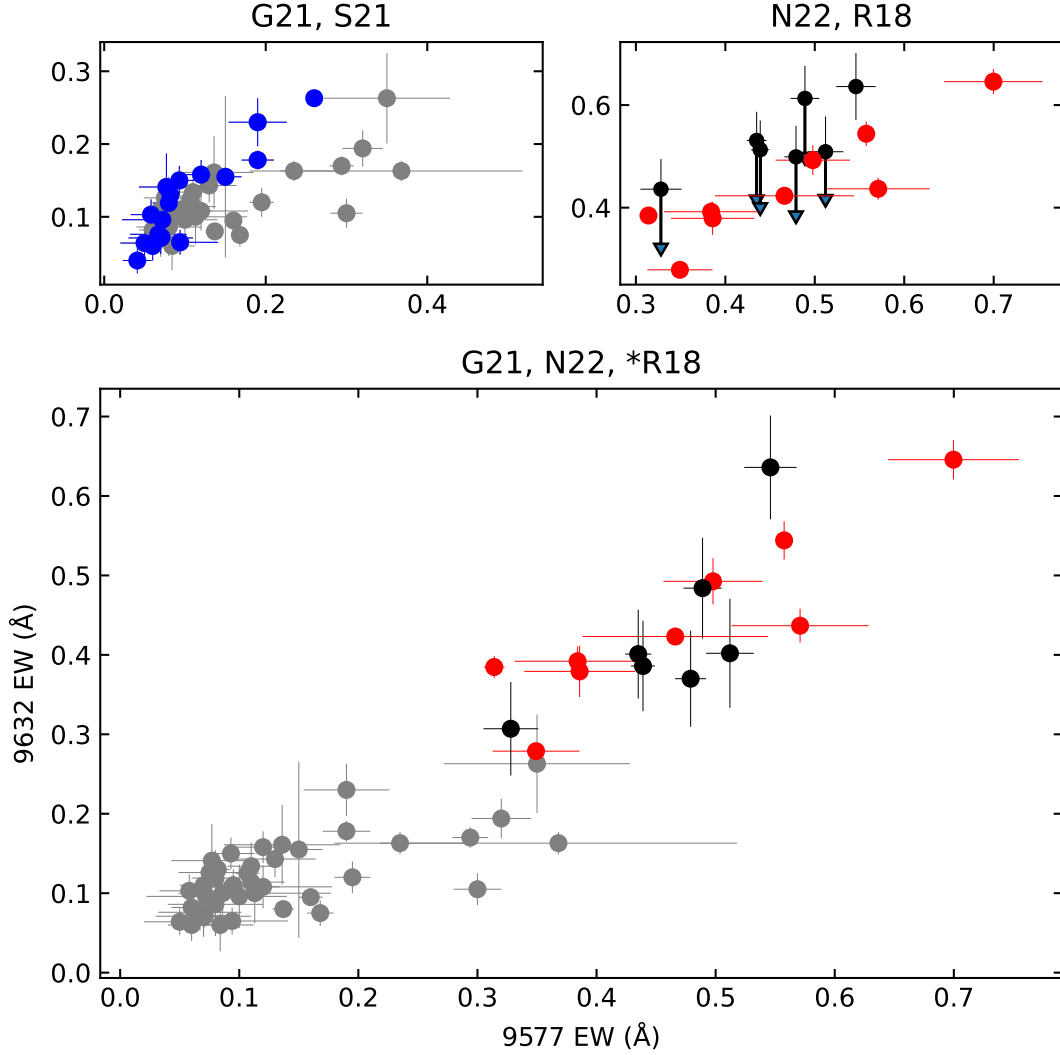


**Figure 1.** DIBs 9577 and 9632 Å are characterized by a high correlation across a sizable  $\simeq 650$  mÅ EW baseline ( $r = 0.93 \pm 0.02$ , G21, N22, \*R18). References correspond to Galazutdinov et al. (2021, gray), Schlarmann et al. (2021, blue), and Nie et al. (2022, red). Advantageous higher EW sightlines were added from Ramírez-Tannus et al. (2018, black) since they mostly do not overlap with Nie et al. (2022), and were adjusted here for stellar Mg II contamination (bottom panel, \*R18, see text). Arrows in the top right panel convey the Mg II corrections. Table 1 highlights the dependence of  $r$  and the slope on permutations of the underlying data.

2019), although here too the conclusion is contested (Galazutdinov et al. 2021).

The topic is pertinent since  $C_{60}^+$  is hitherto the sole carrier of DIBs where a consensus is coalescing (e.g., Cordiner et al. 2019; Nie et al. 2022). Several hundred other DIBs remain unassociated with specific molecules. Majaess et al. (*submitted*) advocated that the signatures of

C–H, C=O,  $C\equiv C$ ,  $C\equiv N$ , S–H, and aromatics (=C–H stretch, out of plane C–H bending, in-ring  $C\equiv C$ , overtones) are discernible in energy differences between correlated DIBs in the APO catalog (Fan et al. 2019). Indeed, PAHs are hypothesized to be leading candidates for DIB sources (e.g., Bondar 2020; Weber et al. 2022), and efforts are likewise ongoing to explore the

viability of fullerenes beyond  $C_{60}^+$  (§2.2), heterofullerenes, and their (endo/exo)hedral inclusions (e.g., [Campbell et al. 2016b](#); [Omont 2016](#)). A subset of those molecules may likewise explain the unidentified infrared emission lines ([Sadjadi et al. 2020, 2022](#)), in addition to MAONs (mixed aromatic/aliphatic organic nanoparticles, [Kwok 2022](#); [Kwok & Sadjadi 2023](#)).

In this study, concerns regarding the correlation between the 9577 and 9632 Å DIBs are assuaged. Furthermore, additional DIBs are inspected whose source may also be connected to fullerenes (i.e.,  $C_{70}^+$  and  $C_{70}^{2+}$ ), given tightly constrained matching wavelengths *vis à vis* laboratory results ([Campbell et al. 2016b, 2017](#)).

## 2. ANALYSIS

### 2.1. $C_{60}^+$ : 9577 and 9632 Å

[Galazutdinov et al. \(2021\)](#) concluded that the correlation between 9577 and 9632 Å is  $r = 0.37$ , whereas [Schlarmann et al. \(2021\)](#) favored estimates spanning 0.82–0.93. [Nie et al. \(2022\)](#) inspected separate stars featuring higher EWs and advocated that  $r = 0.89 - 0.96$ .

It is argued here that the ambiguity partly arises from not bridging the analysis over a sizable EW baseline, whereby [Galazutdinov et al. \(2021\)](#) and [Schlarmann et al. \(2021\)](#) sample relatively low EWs, [Nie et al. \(2022\)](#) data reside within a higher EW domain, and linking the datasets reveals a robust high correlation between 9577 and 9632 Å (Fig. 1, Table 1). [Schlarmann et al. \(2021, their Table 1\)](#) relied principally on [Galazutdinov et al. \(2021\)](#) data (Fig. 1, top left panel), and consequently the former is omitted from the final correlation determination (bottom panel of Fig. 1,  $r = 0.93 \pm 0.02$ ).

Permutations of the datasets in concert with their slope and correlation determinations are conveyed in Table 1, which stemmed from an unweighted evaluation since the uncertainties are inhomogeneous. A firm high correlation

**Table 1.** Correlation and slope for 9577-9632 Å.

Datasets	$r \pm \Delta r$	$m \pm \Delta m$
G21, N22	$0.92 \pm 0.02$	$0.80 \pm 0.04$
S21, N22	$0.98 \pm 0.01$	$0.82 \pm 0.05$
G21, *R18	$0.89 \pm 0.03$	$0.77 \pm 0.06$
S21, *R18	$0.96 \pm 0.02$	$0.86 \pm 0.05$
G21, N22, *R18	$0.93 \pm 0.02$	$0.83 \pm 0.04$
S21, N22, *R18	$0.97 \pm 0.01$	$0.86 \pm 0.04$
G21, S21, N22, *R18	$0.94 \pm 0.01$	$0.83 \pm 0.04$

Notes: references are [Galazutdinov et al. \(2021, G21\)](#), [Schlarmann et al. \(2021, S21\)](#), and [Nie et al. \(2022, N22\)](#). Sightlines linked to comparatively cooler stars were added since they are mostly not featured in the other datasets, and once corrected for stellar Mg II contamination ([Ramírez-Tannus et al. 2018, \\*R18](#)) (see text).

remains in the absence of the [Schlarmann et al. \(2021\)](#) data, or the adjusted [Ramírez-Tannus et al. \(2018\)](#) findings (Table 2). Regarding the latter, pertinent high EW datapoints were added from [Ramírez-Tannus et al. \(2018\)](#) once their uncorrected 9632 Å EWs were adjusted for stellar Mg II contamination. Those stars largely differ from the subsample presented by [Nie et al. \(2022\)](#) (B215 overlaps), who focused on hotter stars to mitigate the impact of Mg II. Tables 1 and 2 in [Galazutdinov et al. \(2017\)](#) include corrections for stars spanning diverse parameters (e.g.,  $T_{\text{eff}}$ , metallicity,  $v_T$ ,  $\log g$ ), and a sigmoid was applied to approximate an upper bound Mg II– $T_{\text{eff}}$  relation over the baseline examined:  $\Delta EW \approx (130 \pm 50 \text{ mÅ})(1 - (1 + e^{(20200 - T_{\text{eff}})/1751})^{-1})$ . Corrections emerging from that approximation were subsequently applied to the seven stars using spectral types from [Ramírez-Tannus et al. \(2017, 2018\)](#),<sup>1</sup> and their corresponding tem-

<sup>1</sup> A B8 temperature class was assumed when [Ramírez-Tannus et al. \(2018\)](#) relayed a ‘late-B’ classification.

peratures stemmed from unpublished data by D. G. Turner (e.g., used in [Turner 1994](#), and references therein). Uncertainties for the corrected 9632 Å [Ramírez-Tannus et al. \(2018\)](#) EWs were all expanded in quadrature by a bulk 50 mÅ from their original values. Table 2 underscores that the corrections shift the original [Ramírez-Tannus et al. \(2018\)](#) data downward in Fig. 1 (top right panel) and upon the [Nie et al. \(2022\)](#) observations. Otherwise, the initial [Ramírez-Tannus et al. \(2018\)](#) EWs are too high, and discernibly offset from the [Nie et al. \(2022\)](#) data. As noted [Nie et al. \(2022\)](#) do not require corrections owing to their hotter temperature sample. That in sum reaffirms that the approximated Mg II corrections are satisfactory for the present purpose, despite the uncertainties (e.g., deviations from the mean trend, SpT,  $T_{\text{eff}}$ , possible Doppler offsets between Mg II and the DIB, and for the latter see Fig. 4 in [Galazutdinov et al. 2017](#)). [Lallement et al. \(2018\)](#) and [Galazutdinov et al. \(2021\)](#) debated the Mg II corrections employed by [Galazutdinov et al. \(2017\)](#), and for additional approaches to the problem consider [Jenniskens et al. \(1997\)](#) and [Walker et al. \(2016\)](#). A comprehensive spectral analysis comparing differing atmospheric models is desirable but beyond the scope of this current effort, especially given the scaffolding underpinning Table 1 and the consistently high correlation conclusion.

## 2.2. The $C_{70}^+$ and $C_{70}^{2+}$ DIB families

There may be DIBs tied to other fullerenes (e.g.,  $C_{70}^+$ ,  $C_{70}^{2+}$ , Table 3). Those lines could help demarcate mid-infrared vibrations, whereby energy differences among DIBs within the family (e.g., highly correlated EWs) could represent separate vibrational modes. Experimental wavelengths for  $C_{70}^+$  and  $C_{70}^{2+}$  were adopted from [Campbell et al. \(2016b, 2017\)](#), and compared

**Table 2.** [Ramírez-Tannus et al. \(2018\)](#) original and corrected 9632 Å EWs.

ID	SpT	EW <sub>0</sub> (mÅ)	EW <sub>c</sub> (mÅ)
B215	B0-B1V	636±42	636±65
B243	B8V	499±34	370±60
B253	B3-B5III	509±47	402±69
B268	B9-A0	531±25	401±56
B275	B7III	513±27	386±57
B331	late-B	436±31	307±59
B337	late-B	613±39	484±63

Notes: IDs and spectral types stem from [Ramírez-Tannus et al. \(2018\)](#). Their 9632 Å EWs were corrected (EW<sub>c</sub>) for stellar Mg II contamination (see text). A high correlation between 9632 and 9577 Å persists in the absence of the aforementioned data (Table 1).

**Table 3.** *Candidate* fullerene DIBs.

DIB (Å)	$\lambda_e$ (Å)	Ion	$\lambda_e$ (ref.)
7470.38	7470.2	$C_{70}^+$	<a href="#">Campbell et al. 2016b</a>
7558.44	7558.4	$C_{70}^+$	<a href="#">Campbell et al. 2016b</a>
7581.47	7582.3	$C_{70}^+$	<a href="#">Campbell et al. 2016b</a>
6926.48	6927	$C_{70}^{2+}$	<a href="#">Campbell et al. 2017</a>
7030.26	7030	$C_{70}^{2+}$	<a href="#">Campbell et al. 2017</a>

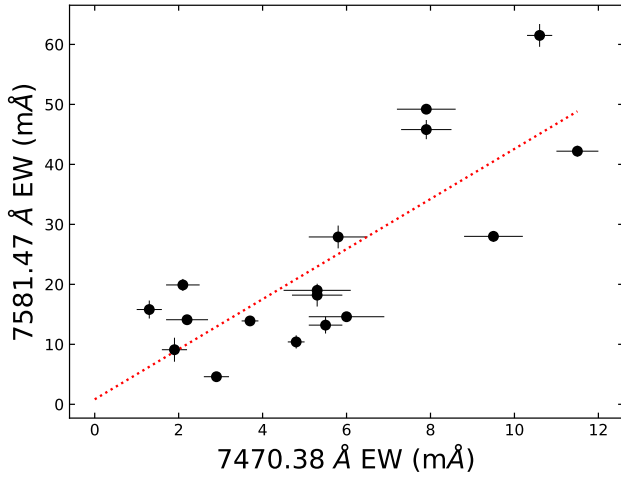
Notes: DIB wavelengths stem from the APO catalog ([Fan et al. 2019](#)), save 7558.44 Å ([Jenniskens & Desert 1994](#); [Hobbs et al. 2009](#), see text).  $\lambda_e$  are experimental wavelengths ([Campbell et al. 2016b, 2017](#)).

to published DIB wavelengths ([Jenniskens & Desert 1994](#); [Hobbs et al. 2009](#); [Bondar 2012](#); [Fan et al. 2019](#)). For  $C_{70}^+$  the following DIBs align with experimental results to within 1 Å: 7470.38, 7558.44, and 7581.47 Å. [Campbell et al. \(2016b\)](#) relay that the most prominent laboratory  $C_{70}^+$  line (7632.6 Å) shall be severely

**Table 4.** DIB correlations, slopes, and lab attenuation ratios.

DIB (Å)	$\overline{EW}$ (mÅ)	DIB (Å)	$n$	$r$ $\pm\Delta r$	$m$ $\pm\Delta m$	$R_a$ $\pm\Delta R_a$
$C_{70}^+$						
7470.38	6	7557.88	12	0.84 $\pm 0.10$	2.6 $\pm 0.5$	1.0 $\pm 0.3$
7470.38	5	7581.47	17	0.80 $\pm 0.10$	4.2 $\pm 0.8$	1.3 $\pm 0.4$
7557.88	12	7581.47	14	0.76 $\pm 0.13$	1.6 $\pm 0.4$	1.3 $\pm 0.4$
$C_{70}^{2+}$						
6926.48	4	7030.26	9	0.84 $\pm 0.12$	0.8 $\pm 0.2$	2.0 $\pm 0.6$

Notes: DIB wavelengths and EWs from the APO catalog (Fan et al. 2019). Low statistics and EWs, and a limited baseline, suggest the uncertainty is larger than cited.

**Figure 2.** Correlation analysis between two DIBs (7470.38 – 7581.47 Å) which exhibit wavelengths comparable to experimental  $C_{70}^+$  lines (Table 3). The expected low EWs ( $\lambda_e = 7470.38$  Å, Campbell et al. 2016b) help expand the correlation uncertainty ( $r = 0.80 \pm 0.10$ ). The slope ( $m = 4.2 \pm 0.8$ ) is larger than an indirect comparison to the relative lab-measured attenuation ( $R_a$ , Table 4).

contaminated by telluric absorption, and hence the motivation for satellite measurements (e.g., Cordiner et al. 2019). Furthermore, APO catalog DIBs linked to 6926.48 and 7030.26 Å may be indicative of  $C_{70}^{2+}$ , again owing to their wavelength proximity relative to experimental determinations (Campbell et al. 2017). Regarding the Campbell et al. (2016b) laboratory  $C_{70}^+$  wavelength at  $\lambda_e = 7558.4$  Å, Jenniskens & Desert (1994) and Bondar (2012) feature DIBs at 7558.5 and 7559.19 Å, respectively. That is supported by Hobbs et al. (2009), who characterized DIBs at 7558.44 and 7559.48 Å, with the former being numerically coincident with the experimental result of 7558.4 Å (Table 3). The Fan et al. (2019) compilation possesses lines bracketing the laboratory measurement at 7557.88 and 7559.43 Å, which in tandem with the aforementioned Hobbs et al. (2009) DIBs, could represent the same vibrational line with differing rotation.<sup>2</sup>

An effort was undertaken to (in)validate the wavelength analysis by one tied to correlations (Table 4). EWs and wavelengths were adopted from Fan et al. (2019) given their sample size (i.e., number of sightlines  $n \geq 9$ ). Unweighted correlations that emerged include  $r = 0.84 \pm 0.10$  for the 7470.38 – 7557.88 Å DIB pair (Table 4), and  $r = 0.80 \pm 0.10$  for 7470.38 – 7581.47 Å (Fig. 2). The correlation evaluations are merely suggestive owing partly to the impact on uncertainties from expectedly<sup>3</sup> low EWs (e.g., 7470.38 Å has a median  $\overline{EW} = 5$  mÅ). That uncertainty likewise complicates a comparison between low interstellar EWs and relative laboratory attenuation ( $R_a$ , Table 4), which measure separate marginal (in this instance) quantities in differing environments. For example, experiments implied that  $\lambda_e = 7470.2$  Å exhibits a

<sup>2</sup> That may likewise be true of the Fan et al. (2019) 5779.59 and 5780.64 Å DIBs (Smith et al. 2021).

<sup>3</sup> Campbell et al. (2016b, 2017).



lower intensity than 7582.3 Å (Campbell et al. 2016b), and that is apparent in Fig. 2. The slope characterizing those DIB EWs ( $m = 4.2 \pm 0.8$ ) is larger than an indirect comparison to the relative lab-measured attenuation ( $R_a \sim 1.3$ ). As noted above, it is also unclear whether the highly correlated APO catalog lines of 7557.88 and 7559.43 Å ( $r = 0.92 \pm 0.05$ ,  $n = 16$ ) constitute a single vibrational line, and the EWs must be combined prior to a comparison with experimental results. Additional observations across a sizable EW baseline may clarify whether the DIBs belong to fullerene carriers, or represent a numerical coincidence. Yet reliably measuring such low EWs poses a challenge, especially given the experimental FWHM, as noted previously (Campbell et al. 2016b, 2017).

### 3. CONCLUSIONS

DIBs linked to the buckminsterfullerene cation at 9577 and 9632 Å are highly correlated (Fig. 1,  $r = 0.93 \pm 0.02$ ). That assessment stemmed from an analysis spanning a lucrative EW baseline, and bridging low to high EWs provides a confident conclusion. The EWs were tied to existing (Galazutdinov et al. 2021; Nie et al. 2022) and newly corrected estimates (Ramírez-Tannus et al. 2018). Regarding the

latter, 9632 Å datapoints linked to relatively cooler stars within Ramírez-Tannus et al. (2018) were corrected here for Mg II contamination (top right panel of Fig. 1). Their addition reaffirms the overarching conclusion of a high Pearson correlation (Table 1).

The analysis was expanded to identify DIBs associated with fullerenes beyond  $C_{60}^+$  (i.e.,  $C_{70}^+$  and  $C_{70}^{2+}$ ). Several DIBs overlap with the Campbell et al. (2016b, 2017) laboratory wavelengths to within an Angstrom (Table 3, e.g., DIB 7558.44 Å and  $C_{70}^+ \lambda_e = 7558.4$  Å). A complementary correlation analysis was limited by low EWs and statistics (Fig. 2, Table 4, e.g.,  $\overline{EW} = 4$  mÅ for 6926.48 Å). Additional observations over an extensive EW baseline are required to assess whether those DIBs are linked to fullerene cations. The current evidence, though inconclusive, provides sufficient impetus to pursue such observations. Future work may include relinquishing a strict  $< 1$  Å criterion, and exploring matches relative to fractionary offsets within a FWHM (e.g.,  $|\text{DIB} - \lambda_e| < \frac{1}{x} \text{FWHM}$ ).

This research relied on initiatives such as Campbell et al., APO Catalog of DIBs, CDS, NASA ADS, arXiv.

### REFERENCES

- Bondar, A. 2012, MNRAS, 423, 725,  
doi: [10.1111/j.1365-2966.2012.20910.x](https://doi.org/10.1111/j.1365-2966.2012.20910.x)  
—, 2020, MNRAS, 496, 2231,  
doi: [10.1093/mnras/staa1610](https://doi.org/10.1093/mnras/staa1610)  
Campbell, E. K., Holz, M., Gerlich, D., & Maier, J. P. 2015, Nature, 523, 322,  
doi: [10.1038/nature14566](https://doi.org/10.1038/nature14566)  
Campbell, E. K., Holz, M., & Maier, J. P. 2016a, ApJL, 826, L4,  
doi: [10.3847/2041-8205/826/1/L4](https://doi.org/10.3847/2041-8205/826/1/L4)  
—, 2017, ApJ, 835, 221,  
doi: [10.3847/1538-4357/835/2/221](https://doi.org/10.3847/1538-4357/835/2/221)  
Campbell, E. K., Holz, M., Maier, J. P., et al. 2016b, ApJ, 822, 17,  
doi: [10.3847/0004-637X/822/1/17](https://doi.org/10.3847/0004-637X/822/1/17)  
Cordiner, M. A., Linnartz, H., Cox, N. L. J., et al. 2019, ApJL, 875, L28,  
doi: [10.3847/2041-8213/ab14e5](https://doi.org/10.3847/2041-8213/ab14e5)  
Fan, H., Hobbs, L. M., Dahlstrom, J. A., et al. 2019, ApJ, 878, 151,  
doi: [10.3847/1538-4357/ab1b74](https://doi.org/10.3847/1538-4357/ab1b74)  
Fulara, J., Jakobi, M., & Maier, J. P. 1993, Chemical Physics Letters, 211, 227,  
doi: [10.1016/0009-2614\(93\)85190-Y](https://doi.org/10.1016/0009-2614(93)85190-Y)  
Galazutdinov, G. A., Shimansky, V. V., Bondar, A., Valyavin, G., & Krelowski, J. 2017, MNRAS, 465, 3956,  
doi: [10.1093/mnras/stw2948](https://doi.org/10.1093/mnras/stw2948)

- Galazutdinov, G. A., Valyavin, G., Ikhsanov, N. R., & Krelowski, J. 2021, *AJ*, 161, 127, doi: [10.3847/1538-3881/abd4e5](https://doi.org/10.3847/1538-3881/abd4e5)
- Hobbs, L. M., York, D. G., Thorburn, J. A., et al. 2009, *ApJ*, 705, 32, doi: [10.1088/0004-637X/705/1/32](https://doi.org/10.1088/0004-637X/705/1/32)
- Jenniskens, P., & Desert, F. X. 1994, *A&AS*, 106, 39
- Jenniskens, P., Mulas, G., Porceddu, I., & Benvenuti, P. 1997, *A&A*, 327, 337
- Kwok, S. 2022, *Ap&SS*, 367, 16, doi: [10.1007/s10509-022-04045-6](https://doi.org/10.1007/s10509-022-04045-6)
- Kwok, S., & Sadjadi, S. 2023, in *American Astronomical Society Meeting Abstracts*, Vol. 241, American Astronomical Society Meeting Abstracts, 144.07
- Lallement, R., Cox, N. L. J., Cami, J., et al. 2018, *A&A*, 614, A28, doi: [10.1051/0004-6361/201832647](https://doi.org/10.1051/0004-6361/201832647)
- Nie, T. P., Xiang, F. Y., & Li, A. 2022, *MNRAS*, 509, 4908, doi: [10.1093/mnras/stab3296](https://doi.org/10.1093/mnras/stab3296)
- Omont, A. 2016, *A&A*, 590, A52, doi: [10.1051/0004-6361/201527685](https://doi.org/10.1051/0004-6361/201527685)
- Ramírez-Tannus, M. C., Cox, N. L. J., Kaper, L., & de Koter, A. 2018, *A&A*, 620, A52, doi: [10.1051/0004-6361/201833340](https://doi.org/10.1051/0004-6361/201833340)
- Ramírez-Tannus, M. C., Kaper, L., de Koter, A., et al. 2017, *A&A*, 604, A78, doi: [10.1051/0004-6361/201629503](https://doi.org/10.1051/0004-6361/201629503)
- Sadjadi, S., Kwok, S., Cataldo, F., García-Hernández, D. A., & Manchado, A. 2020, *Fullerene Nanotubes and Carbon Nanostructures*, 28, 637, doi: [10.1080/1536383X.2020.1731735](https://doi.org/10.1080/1536383X.2020.1731735)
- Sadjadi, S., Parker, Q. A., Hsia, C.-H., & Zhang, Y. 2022, *ApJ*, 934, 75, doi: [10.3847/1538-4357/ac75d5](https://doi.org/10.3847/1538-4357/ac75d5)
- Schlarmann, L., Foing, B., Cami, J., & Fan, H. 2021, *A&A*, 656, L17, doi: [10.1051/0004-6361/202142669](https://doi.org/10.1051/0004-6361/202142669)
- Smith, F. M., Harriott, T. A., Majaess, D., Massa, L., & Matta, C. F. 2021, *MNRAS*, 507, 5236, doi: [10.1093/mnras/stab2444](https://doi.org/10.1093/mnras/stab2444)
- Turner, D. G. 1994, *JRASC*, 88, 176
- Walker, G. A. H., Campbell, E. K., Maier, J. P., Bohlender, D., & Malo, L. 2016, *ApJ*, 831, 130, doi: [10.3847/0004-637X/831/2/130](https://doi.org/10.3847/0004-637X/831/2/130)
- Weber, I., Tsuge, M., Sundararajan, P., et al. 2022, *Journal of Physical Chemistry A*, 126, 5283, doi: [10.1021/acs.jpca.2c02906](https://doi.org/10.1021/acs.jpca.2c02906)